Cethrene: The Chameleon of Woodward–Hoffmann Rules

Šolomek, Tomáš ; Ravat, Prince ; Mou, Zhongyu ; Kertesz, Miklos ; Juríček, Michal

Abstract: We demonstrate that the electrocyclic (EC) ring-closure of cethrene in solution proceeds in a conrotatory mode both thermally and photochemically. The facile photochemical EC process promises that cethrene can serve as an efficient chiroptical switch operated solely by light. As for the thermally activated EC reaction, a low reaction barrier and a solvation effect on the EC rate indicate that the C2-symmetric pathway predicted by DFT calculations might not be the correct mechanism. Instead, we argue that the molecular symmetry decreases along the reaction coordinate as a consequence of the low-energy singlet excited state in this diradicaloid molecule, which might lead to a lower activation energy in accord with that determined through kinetic studies. Cethrene, therefore, represents a thought-provoking molecular chameleon of the Woodward–Hoffmann rules that puts our chemical concepts and intuition to test.

DOI: https://doi.org/10.1021/acs.joc.8b00656

JOC The Journal of Organic Chemistry

Cethrene: The Chameleon of Woodward–Hoffmann Rules

Tomas Solomek, Prince Ravat, Zhongyu Mou, Miklos Kertesz, and Michal Juricek

J. Org. Chem., **Just Accepted Manuscript** • Publication Date (Web): 19 Mar 2018

Just Accepted

ACS Publications

is published by the American Chemical Society. 1155 Sixteenth Street N.W., Washington, DC 20036

Cethrene: The Chameleon of Woodward–Hoffmann Rules

Tomáš Šolomek,*[,†] Prince Ravat,[†,‡] Zhongyu Mou,[§] Miklos Kertesz,[§] and Michal Juríček*[,†,∥]

[†]Department of Chemistry, University of Basel, St. Johanns-Ring 19, CH-4056 Basel, Switzerland

[‡]Department of Chemistry, The University of Tokyo, 7-3-1 Hongo, Bunkyo-ku, Tokyo 113-0033, Japan

[§]Department of Chemistry and Institute of Soft Matter, Georgetown University, 37th and O Streets Washington, DC 20057-1227, United States

[∥]Department of Chemistry, University of Zurich, Winterthurerstrasse 190, CH-8057 Zurich, Switzerland

In memory of Pavel Kubáček (1947–2017), an Associate Professor at Masaryk University, Czech Republic and a former postdoctoral fellow in the laboratory of Professor Roald Hoffmann.

ABSTRACT: We demonstrate that the electrocyclic (EC) ring-closure of cethrene in solution proceeds in a conrotatory mode both thermally and photochemically. The facile photochemical EC process promises that cethrene could serve as an efficient chiroptical switch operated solely by light. As for the thermally activated EC reaction, a low reaction barrier and a solvation effect on the EC rate indicate that the C_2-symmetric pathway predicted by DFT calculations might not be the correct mechanism. Instead, we argue that the molecular symmetry decreases along the reaction coordinate as a consequence of the low-energy singlet excited state in this diradicaloid molecule, which might lead to a lower activation energy in accord with that determined through kinetic studies. Cethrene therefore represents a thought-provoking molecular chameleon of the Woodward–Hoffmann rules that puts our chemical concepts and intuition to test.

TABLE OF CONTENTS

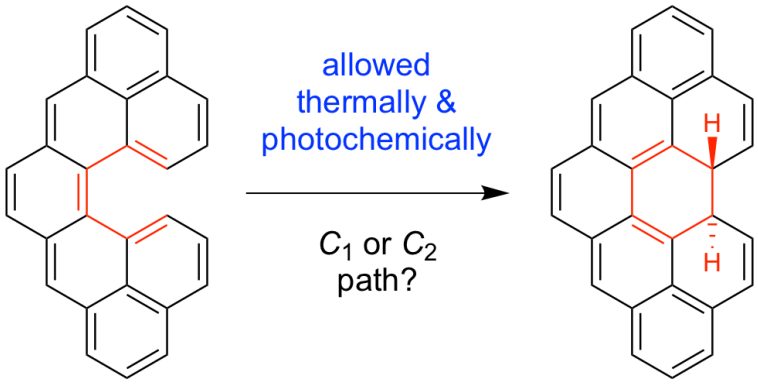

INTRODUCTION

The ability of chemists to predict the outcome of an organic reaction is perhaps best illustrated by the case of pericyclic reactions.[1] The stereochemical result of these concerted transformations can be determined through analysis of the symmetry of the frontier molecular orbitals (FMOs), which is commonly known as the Woodward–Hoffmann rules (WHr).[2] A classic example of a pericyclic reaction is a ring-opening of 3,4-dimethylcyclobutene[3] (Scheme 1a), which belongs to the category of electrocyclic (EC) reactions.[4] In accord with WHr (Scheme 1b), the thermal ring-opening does not proceed in a disrotatory but a conrotatory mode, that is, the *cis*-isomer gives the (*E*,*Z*)-product. The disrotatory mode is favored when this reaction proceeds photochemically and the *cis*-isomer gives the (*E*,*E*)-product.

As it is often the case, there are exceptions to these rules and reactions, which do not conform to WHr, do exist. These include thermal EC reactions, which proceed via symmetry-forbidden pathways[5–7] on account of steric constraints. Considering their forbidden nature, these reactions can have surprisingly low activation energies, as a result of various factors such as a release of steric strain[6] or a gain of aromatic stabilization energy.[7] In addition to cases when it is apparent whether a reaction is symmetry-allowed or not, situations may arise, when it is puzzling to decide, whether a reaction does or does not conform to WHr. These include singlet diradicaloid molecules,[8–10] which are characterized by low HOMO–LUMO gaps, resulting in a distribution of two electrons between the FMOs or, in other words, HOMO and LUMO being *both* partially occupied in the ground state. As a result, a formally "forbidden" rotatory mode becomes "allowed" and such "chameleonic" reaction can proceed via this mode both thermally and photochemically. The first example of this kind was described[8] by Michl and co-workers, who reported an EC ring-closing reaction of a dimethyl derivative of pleiadene **1** (Scheme 1c), incorporating a 1,4-dimethylbuta-1,3-diene unit (in

red). This reaction has three unique features: it proceeds (1) in the opposite direction compared to the reaction of 3,4-dimethylcyclobutene (gain of aromatic stabilization energy "pays" the cost of creating strain), (2) in a disrotatory mode because of steric constraints, and (3) with an unusually low activation energy, considering it is formally a "symmetry-forbidden" process. It was reasoned that the low-lying first doubly excited state of this diradicaloid molecule might account for why there would not be a *"great sacrifice involved in reaching the "forbidden" transition state"*.[8a]

Scheme 1. Examples of Electrocyclic (EC) Reactions (a, c) and Corresponding FMO-Symmetry Considerations (b)

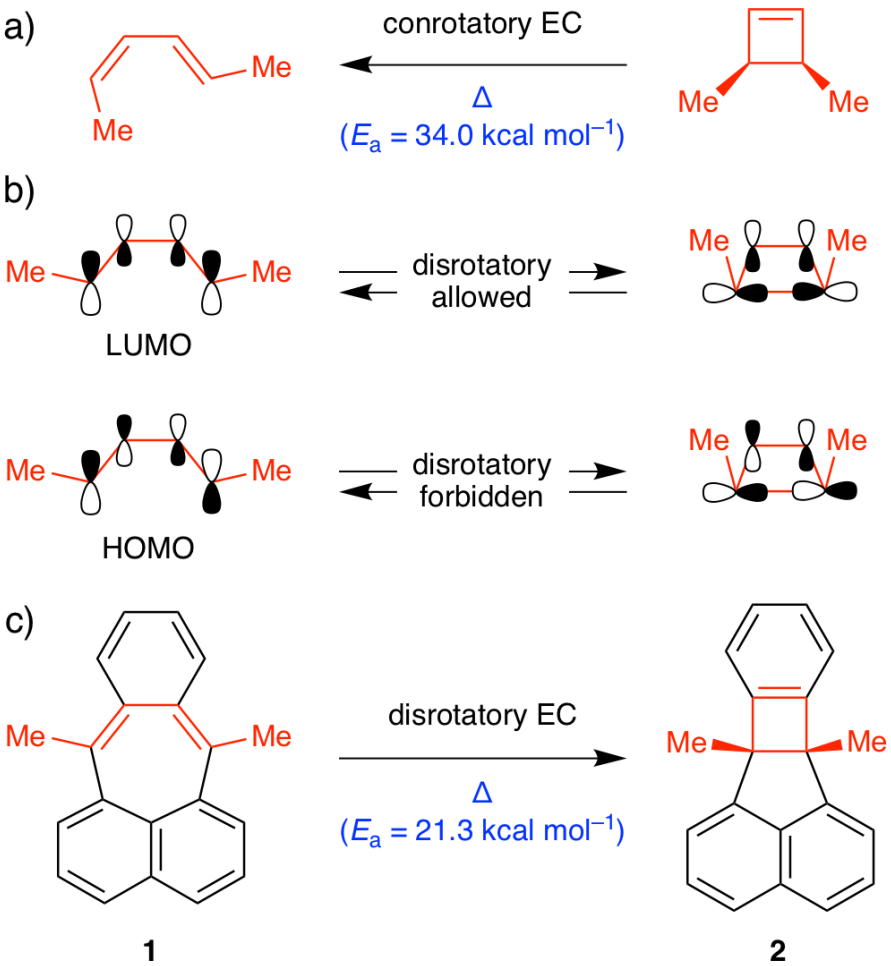

Recently, we have synthesized a diphenyl derivative **3b** (R = Ph) of a helical diradicaloid hydrocarbon cethrene[11] (**3a**, R = H) and observed[11b] that it undergoes a facile transformation to a planar hydrocarbon **4b** (R = Ph) at temperatures below ambient (Scheme 2a,b). Although we could not observe the intermediate of the conrotatory EC ring-closure (*anti*-**5b**, R = Ph), we hypothesized that this would be the first step of the transformation of **3b** to **4b**. The second step would be the oxidation of *anti*-**5b** to **4b** by oxygen or oxidant *p*-chloranil. This hypothesis was later supported[10a] by the recent work of Kubo and co-workers, who gathered experimental evidence that the (*Z*)-isomer of biphenalenylidene, (*Z*)-**6**, a close analog of **3**, does undergo the thermal conrotatory EC ring-closure to afford *anti*-**7**, which was isolated and the structure of which was confirmed by NMR and XRD analyses (Scheme 2c).

The EC ring-closures of **3b** and (*Z*)-**6** display similar features to that of **1**: (1) one mode of the reaction is sterically favored over another, in this case, conrotation over disrotation on account of the helical geometry and (2) thermal reaction proceeds via a formally forbidden (conrotatory) mode with low activation energy. For thermal EC ring-closure of (*Z*)-**6** leading to *anti*-**7**, the activation energy (E_a) was determined to be 15.7 kcal mol^{-1}. Interestingly, although this reaction is formally allowed photochemically, it did not proceed upon irradiation by light (700 nm) in the solvent matrix, but it could be reversed upon irradiation at 365 nm (Scheme 2c).[10a] Herein, we present experimental and theoretical evidence that EC ring-closure of **3b** proceeds both thermally and photochemically and support of the intermediacy of *anti*-**5b** in the transformation of **3b** to **4b**. This suggests that derivatives of cethrene could serve as chiroptical and magnetic switches that can be operated solely by light. We also demonstrate that DFT fails to describe the transition state that would agree with the experimental kinetic parameters of the EC ring-closure of **3b** that has a surprisingly low activation energy. We propose a new paradigm, which requires that the molecular

symmetry of cethrene decreases along the reaction coordinate to allow for mixing of singly excited configurations into the ground-state wavefunction.

Scheme 2. Electrocyclic (EC) Ring-Closing Reactions of Cethrene (3; a, b) and Biphenalenylidene (6; c)

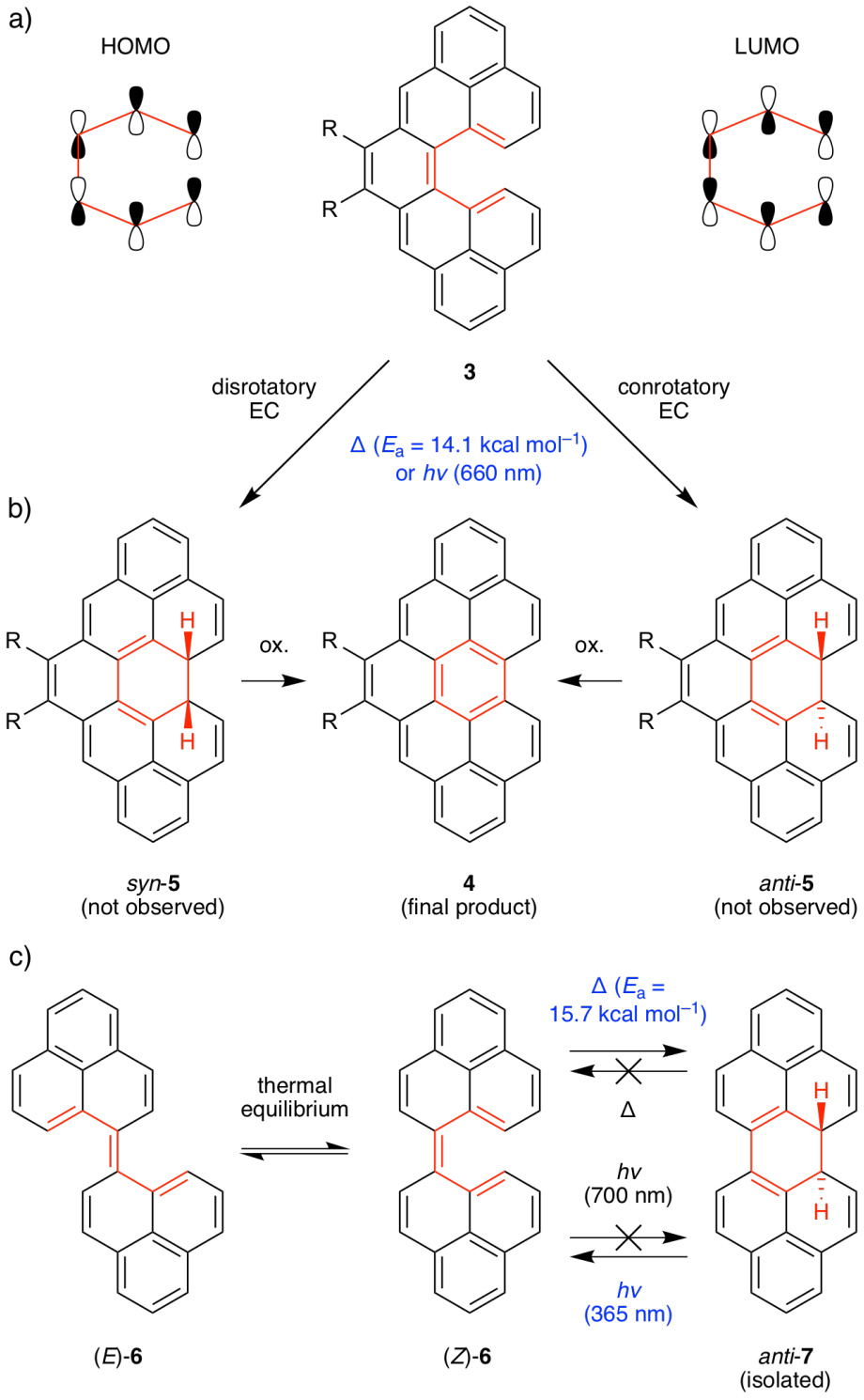

RESULTS AND DISCUSSION

Kinetic Measurements. First, the UV–Vis kinetic studies were performed on **3b** to determine the rate constants (Table S1), at which **3b** reacts to form **4b** at various temperatures. In these studies, the dihydro-precursor of **3b** was treated with 10 equivalents of *p*-chloranil, generating **3b** in situ, which then reacted to form **4b**. The Arrhenius plot allowed us to estimate the activation energy of this process, which was found to be ~14 kcal mol^{-1} (Figure 1). Note that only the absorption bands of **3b** and of **4b** (λ_{max} = 485 nm) could be observed in the UV–Vis spectra in agreement (NMR, UV–Vis) with previous reports.[10a,11b] TD-DFT calculations predict that the first electronic transition (Table S2) in **4a** and *anti*-**5a** occur at comparable energy but that in **4a** displays an oscillatory strength that is 30–160 times higher than that in *anti*-**5a**. We also failed to obtain a spectral signature for this intermediate from the species-associated spectra reconstructed from the global fit of the experimental data with a kinetic model that included the final oxidation step of *anti*-**5b** to form **4b**. Therefore, direct observation of elusive *anti*-**5b** is not possible with UV–Vis measurements. Nevertheless, experimental evidence that **5b** is involved in the transformation of **3b** to **4b** was obtained from irradiation experiments with solutions of **3b**.

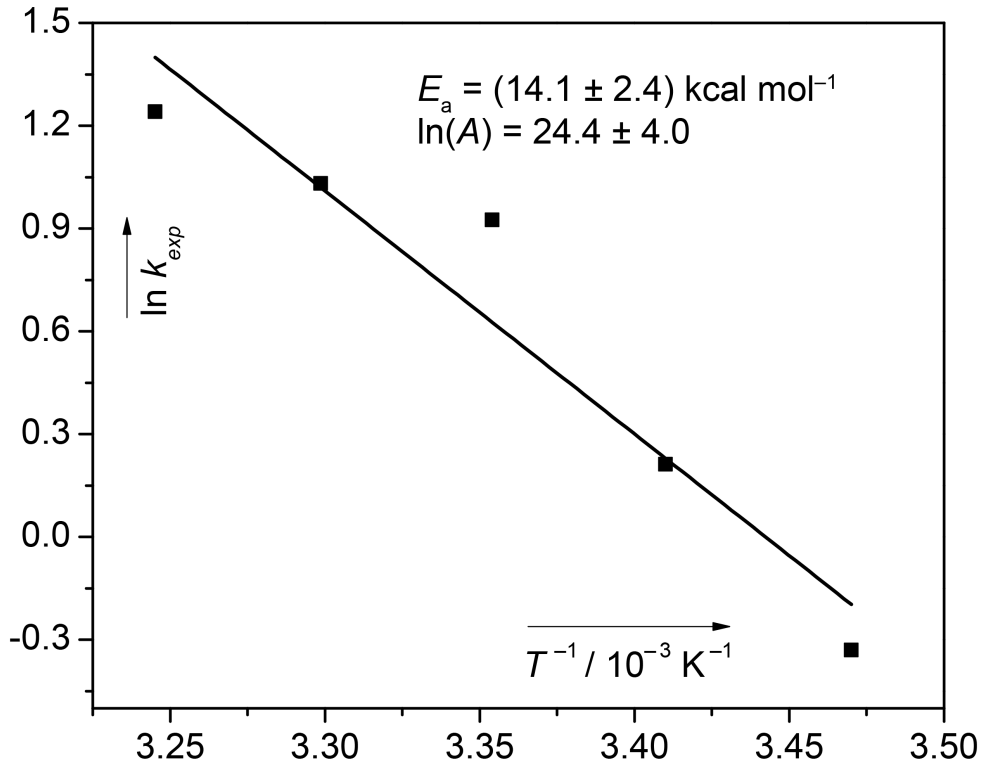

Figure 1. Arrhenius plot of electrocyclization of **3b** in toluene.

Irradiation (λ_{irr} = 660 nm; 30 s) of a solution of **3b** (λ_{max} = 664 nm), generated in situ with three equivalents of *p*-chloranil, led to a jump-change in concentration of **3b** and that of **4b** as evidenced by UV–Vis spectroscopy (Figure 2). While the concentration of **3b** dropped close to zero, that of **4b** significantly increased and continued so for another ~5 minutes in the dark. After this period, the concentration change of **4b** occurred at the rate observed prior to irradiation (Figure S2). When one equivalent of *p*-chloranil was used in the experiment, the subsequent increase in concentration of **4b** after irradiation was accordingly slower. After the irradiation, the concentration of **3b** also gradually increased by further slow oxidation of the dihydro-precursor still present in the solution. Such observations could be done repeatedly (Figure 2) with a given sample, although each consecutive irradiation led to smaller changes in concentrations of **3b** and **4b**.

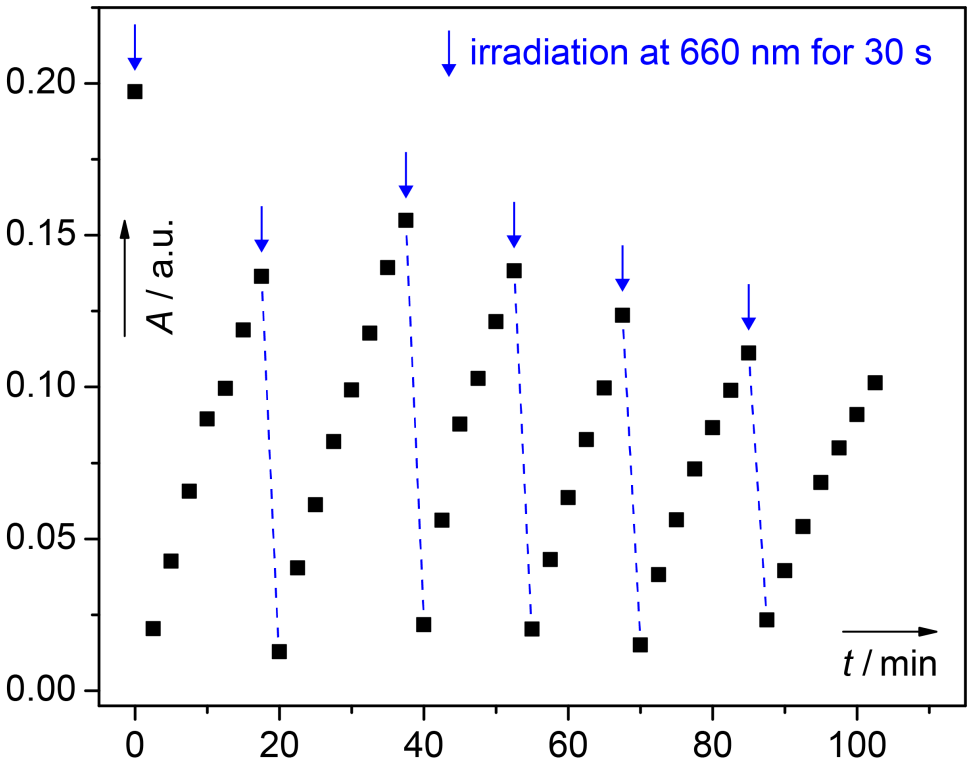

Figure 2. Monitoring of the reaction of dihydro-precursor of **3b** with 3 equiv of *p*-chloranil by UV–Vis spectroscopy at 664 nm in toluene. Blue arrows indicate time-points, when solution was irradiated (660 nm; 30 s) and dashed blue lines illustrate the drop of absorption at 664 nm.

Clearly, the photochemical EC reaction of **3b** in solution does conform to WHr (Scheme 2a) and results in the formation of an intermediate that is directly converted to **4b** with a rate higher than that of thermal EC ring-closure of **3b**, which represents the rate-determining step. Its activation energy is close to that (~16 kcal mol^{-1}) obtained[10a] by Kubo and co-workers for EC ring-closure of (*Z*)-**6**, which suggests that this intermediate is *anti*-**5b**.

DFT Analysis. Our calculations show that the thermally allowed disrotatory EC ring-closure of **3a** to form *syn*-**5a** (R = H) is thermoneutral or slightly endothermic (Table S4) and proceeds through a barrier (~27 kcal mol^{-1}, Table 1) that is higher than that calculated for the

exothermic C_2-symmetric conrotatory EC ring-closure to form *anti*-**5a** (~23 kcal mol^{-1}, Table 1). As in the case of pleiadene **1**,[8] the admixture of a low-lying doubly excited configuration to the ground-state configuration of **3a**, which is accounted for by using broken-symmetry DFT or multireference CASSCF, results in a decrease of the barrier along the C_2-symmetric conrotatory path. The comparable performance of a variety of DFT and wavefunction-based methods to predict this barrier is quite remarkable, but in fact all methods fail when the results are compared to experiment. This discrepancy cannot be explained by a truncated geometry of **3a** used in the calculations because the introduction of the phenyl substituents (**3b**) does not markedly change the EC reaction barrier (see Table S7), solvation (Table S8), enthalpy or entropy considerations (Table S9), or alternative reaction mechanisms involving triplet states (Tables 1, S4, and S6) or radical cations. The latter mechanism is ruled out based on the first oxidation potential of heptazethrene (E_{ox} = 0.17 V vs. Fc^+/Fc in CH_2Cl_2), which is expected to be comparable to the isomeric cethrene, and the first reduction potential of *p*-chloranil (E_{red} = –0.46 V vs. Fc^+/Fc in CH_2Cl_2; $E_{ox} + E_{red}$ = –0.29 V).[12]

Table 1. DFT-Calculated Reaction Barriers[a]

ΔE / kcal mol^{-1}	BLYP	B3LYP	CAM-B3LYP	BMK	M05-2X	M06-2X	M06L
3a$_{RS}$ → *anti*-**5a**	23.6	22.4	18.6	21.7	19.0	22.8	23.0
3a$_{BS}$ → *anti*-**5a**	N/A[b]	23.2	23.1	23.0	21.1	N/A[b]	23.4
3a$_{RS}$ → *syn*-**5a**	27.1	27.4	27.6	27.2	25.8	26.9	28.6
3a$_{BS}$ → *syn*-**5a**	N/A[b]	28.3	32.1	28.5	27.9	N/A[b]	29.1
^{3}**3a** → ^{3}*anti*-**5a**	27.1	30.4	35.3	29.8	–[c]	30.1	27.9

[a] Reaction barriers (in kcal mol^{-1} at 0 K) calculated (cc-pVTZ basis set) with the respective functional on 6-31G(d) geometries with ZPVEs; the transition states are treated with spin-unrestricted (triplets) and spin-unrestricted broken-symmetry (BS, singlets) formalism. The reaction paths to *anti*-**5a** possess C_2 symmetry. [b] Not applicable; no instability was found for the Kohn–Sham wavefunctions computed with the restricted formalism (RS). Energies obtained with the restricted formalism should be used here to compare to other DFT methods. [c] Data not available.

Instead, we offer an explanation that can be particularly relevant to the description of reaction mechanisms involving diradicaloid polycyclic aromatic hydrocarbons in general (Figure 3). From the absorption spectrum of **3b** (Figure S4), we estimate that the lowest singlet excited state of **3b**, configuration of which can be described by a linear combination of two Slater determinants where the HOMO (*a*) and the LUMO (*b*) are occupied by one electron each, is only ~40 kcal mol^{-1} above the ground state. The low energy of such excited state becomes commensurate with the EC activation energy on the C_2-symmetric reaction pathway (see Figure 3a and DFT results) as **3** progresses to the EC product *anti*-**5**, unlike in a typical case where the lowest excited state (or the HOMO–LUMO gap) was high in energy (Figure 3b). The excited-state configuration, however, does not display the proper symmetry (B) that allows for mixing with the totally symmetric (A) ground state configuration. Thus, there will

be a conical intersection within C_2 symmetry, which facilitates the photochemical EC ring-closure of **3**. If this intersection appears much earlier than the avoided crossing between the ground and doubly excited states (Figure 3a), it must be circumvented by a geometry distortion[13] on the thermally activated path from **3** to *anti*-**5**. Consequently, all configurations will belong to the same symmetry and can mix, which will result in decreasing the energy of the C_1-symmetric conrotatory EC transition state (Figure 3a). Note that DFT will fail to describe the proper potential energy surface in such case because it is inherently single-determinantal. Nevertheless, such excited state mixing to recover the necessary electron correlation should be indirect, that is, mediated through double excitations, because the Brillouin's theorem is valid also for the multiconfigurational wavefunctions.[14]

The evidence that supports our hypothesis is as follows: A TD-B3LYP relaxed potential energy surface scan of the S_1 state of **3a** along the EC reaction coordinate leads to a S_1/S_0 surface crossing in C_1 symmetry (black dot, Figure 3a) that we optimized with SA-CASSCF(2,2)/6-31G(d) method. The observed geometry distortion introduces partial charge-transfer character to the wavefunction that must be present also in the EC transition state in C_1 symmetry. The EC ring-closure of **3b** is, therefore, expected to occur faster in a more polar solvent. Indeed, we reported previously that the EC ring-closure of **3b** in dichloromethane is rapid when compared to that in nonpolar toluene or benzene.[11b] Again, the results of our DFT calculations that include the effects of solvation fail to account for such observation (Table S8), which supports that the EC ring-closure of **3b** does not follow the C_2-symmetric pathway.

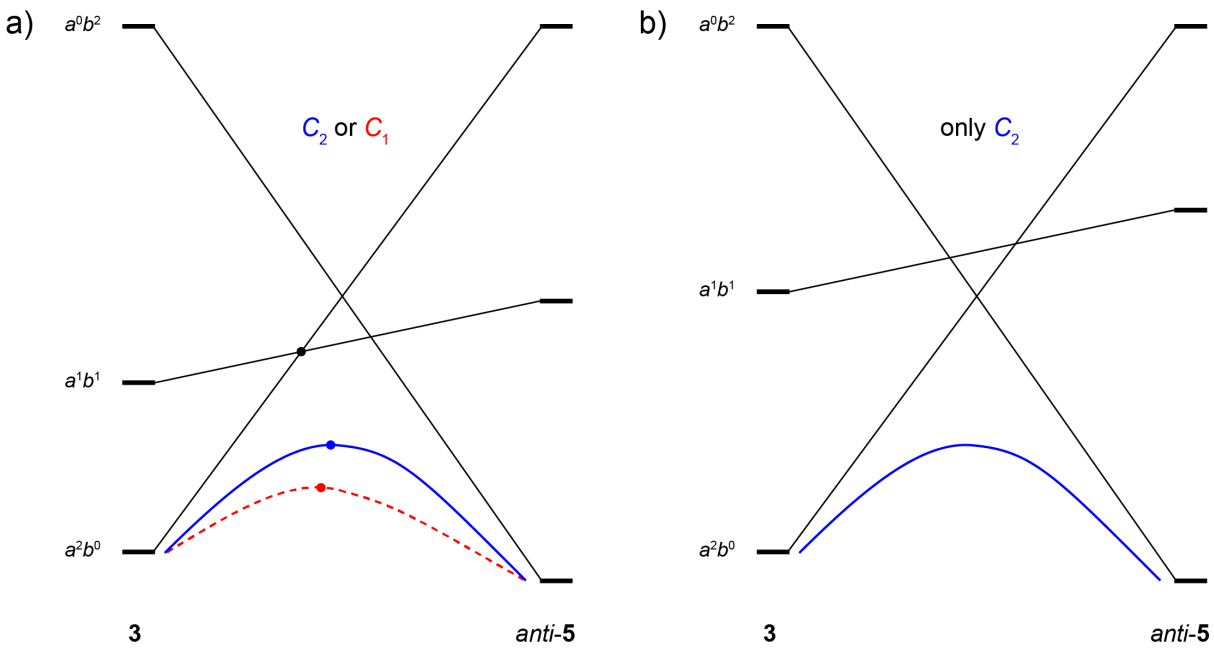

Figure 3. State-correlation diagrams of EC ring-closure of **3** to *anti*-**5** (a = HOMO, b = LUMO) assuming a low (a) and high (b) energy of the lowest singlet excited state in **3**. (a) In C_2 path (blue solid line), a^2b^0 and a^0b^2 configurations mix. In C_1 path (red dashed line), all a^2b^0, a^1b^1, and a^0b^2 configurations can mix. C_2 transition state (blue dot) and S_1/S_0 conical intersection (black dot) were calculated by DFT and CASSCF, respectively. The experimental barrier is highlighted by a red dot. (b) In this case the avoided crossing, a consequence of the symmetry-allowed mixing of the a^2b^0 and a^0b^2 configurations in C_2 path (blue solid line), allows for a smooth passage from **3** to *anti*-**5** with no regard to the presence of the $S_1(a^1b^1)/S_0(a^2b^0 + a^0b^2)$ conical intersection because it is too high in energy. The C_1 path, therefore, does not exist.

Unfortunately, a full description of the potential energy surface of EC ring-closure of **3a** requires repeated numerical calculations of CASSCF Hessian matrix that is beyond our capabilities even with small active spaces for a molecule of size of **3a** in C_1 symmetry.[15] The full understanding of the EC ring-closure of **3b** therefore represents an interesting experimental and computational challenge. The former requires to synthesize chemically

stable models that will allow independent observation of both the open and the closed form of **3**, the control of the lowest-singlet-excited-state energy, and the amount of the charge-transfer character in the wavefunction, while calculations must rely on methods that can sufficiently treat both the non-dynamic and dynamic electron correlation to explore the relevant potential energy surfaces, such as methods similar to CASPT2 quality.

CONCLUSION

We showed the first evidence of the facile photochemical EC ring-closure of cethrene, which together with the photochemical EC ring-opening of the closed form of biphenalenylidene, shown[10a] by Kubo and co-workers, suggests that this type of helical diradicaloid molecules could serve as efficient switches that can be operated solely by light. The thermally and photochemically "allowed" EC ring-closure with respect to the Woodward–Hoffmann rules[2] places cethrene among a rare type of chameleonic molecules such as pleiadene with surprisingly low activation energies of the thermal processes. The description of the EC reaction mechanism by DFT methods fails, however, to reproduce the experimental observations. We argued that the presence of a low-energy conical intersection between the lowest singlet excited state and the ground state forces cethrene to decrease its molecular symmetry along the reaction coordinate and allows to mix the singly excited configurations into the wavefunction. As a consequence, the EC transition state has lower energy and becomes solvent-dependent. The mechanism of such configuration interaction is affected by Brillouin's theorem. Therefore, the complete understanding of the thermal EC process of cethrene represents an interesting experimental and theoretical challenge to test our chemical concepts of pericyclic reactions.

EXPERIMENTAL SECTION

Materials and Instrumentation. HPLC grade toluene and *p*-chloranil were purchased from commercial sources and were used without further purification. Cethrene was prepared in situ in solution by oxidation of its dihydro-precursor with *p*-chloranil. The dihydro-precursor was synthesized as described[11b] previously. The UV–Vis spectra were recorded in toluene with matched 1.00 cm quartz cells. The temperature was controlled by a digital thermostat connected to the sample holder. Irradiation of the samples was conducted using a house-built LED light source equipped with 14 diodes emitting at λ_{em} = (660 ± 10) nm that can be mounted to the sample holder in the UV–Vis spectrophotometer.

Kinetic Measurements. A sample of the dihydro-precursor of cethrene **3b** in toluene was deoxygenated using freeze-pump-thaw technique in three cycles and then treated with 10 equivalents of *p*-chloranil, generating **3b** in situ. The sample was frozen immediately in liquid nitrogen. Before the measurement, the sample was quickly immersed to water with temperature commensurate to that of the sample holder in the UV–Vis spectrophotometer controlled by the thermostat. The sample was then placed to the sample holder and its temperature was equilibrated for 1 min. Visible spectra (540–760 nm) were then recorded as a function of time at 288, 293, 298, 303, and 308 K. Individual kinetic traces were then fitted with a consecutive reactions model where the concentration of **3b** (λ_{max} = 665 nm) initially increased with time ($k_{\mathbf{3b}\text{-form}}$) and diminished ($k_{\mathbf{3b}\text{-dec}}$) later to form the final product **4b** (λ_{max} = 485 nm) that has infinite lifetime. The (pseudo-)first-order kinetic model is expressed with rate matrix *K*:

$$\underline{\underline{K}} = \begin{pmatrix} -k_{3b-form} & 0 & 0 \\ k_{3b-form} & -k_{3b-dec} & 0 \\ 0 & k_{3b-dec} & 0 \end{pmatrix} \qquad \text{(Eq 1)}$$

The rate constants $k_{\mathbf{3b}\text{-dec}}$ obtained from the global fit of the experimental data (Table S1) were then used to construct an Arrhenius plot to determine the barrier associated with electrocyclization of **3b**. The Arrhenius plot is shown in Figures 1 and S1.

Irradiation Experiments. The sample of **3b** in toluene was prepared as described above using 3 equiv of *p*-chloranil. The sample was kept at 288 K and the UV–Vis spectra were taken in constant time intervals (150 s). After an appreciable amount of **3b** formed (15–20 min), the sample was irradiated with a LED light source (λ_{em} = 660 nm) for 30 s. We observed a jump change in absorbance, where that at λ_{max} = 664 nm (Figure 2) dropped nearly to zero, while that at λ_{max} = 486 nm (Figures S2–S5) significantly increased. The absorbance after the irradiation then evolved at a similar rate to that observed prior to the irradiation. Such observation could be done repeatedly with a given sample, although each consecutive irradiation led to smaller changes in absorbance as the dihydro-precursor of **3b** got consumed.

Quantum Chemical Calculations. The DFT calculations were performed in Gaussian 09[16] (Revision D.01) suite of electronic structure programs. The multireference CASSCF calculations were performed in the program MOLPRO[17] (Version 2010.1). The gas-phase geometry optimizations of local energy minima or transition-state structures were done with the respective functional (BLYP, B3LYP, CAM-B3LYP, BMK, M05-2X, M06-2X or M06L) and the 6-31G(d) basis set, and ultrafine integration grid (Integral=Ultrafine keyword in Gaussian). Frequency analysis was performed to test the character of the stationary points and to provide zero-point vibrational energy corrections (ZPVEs), which were used unscaled. The restricted ("R-" prefix) formalism was used to model the singlet states and the unrestricted ("U-" prefix) formalism was used in the modeling of the triplet states. The solution of the SCF equations for the restricted singlet wavefunctions was tested for stability and reoptimized to obtain the lowest energy solution if an RHF→UHF instability was found (Stable=Opt keyword in Gaussian). The broken-symmetry (BS) singlet wavefunction

obtained this way was used to reoptimize the geometries of the molecules. The final gas-phase energies were calculated with the cc-pVTZ basis set. Test calculations revealed that solvation (polarizable continuum model) hardly affected the final relative energies and, therefore, those from the gas-phase calculations are reported. The TD-DFT/6-31G(d) gas-phase calculations served to predict the absorption properties of **4a** and *anti*-**5a**. The seven lowest-energy electronic transitions were calculated and the lowest-energy ones are shown in Table S2.

ASSOCIATED CONTENT

Supporting Information

The Supporting Information is available free of charge on the ACS Publications website.

Details and results of kinetic and computational studies, and Cartesian coordinates of optimized geometries (PDF)

AUTHOR INFORMATION

Corresponding Author

tomas.solomek@unibas.ch

michal.juricek@chem.uzh.ch

Notes

The authors declare no competing financial interest.

ACKNOWLEDGEMENTS

This project has received funding from the European Research Council (ERC) under the European Union's Horizon 2020 research and innovation programme (Grant Agreement No.

716139), the Swiss National Science Foundation (SNSF, T.Š./PZ00P2_174175, M.J./PZ00P2_148043 and PP00P2_170534), the Novartis University of Basel Excellence Scholarship (P.R. and M.J.), and the Experientia Foundation (T.Š.). We gratefully acknowledge the computational facilities of the University of Fribourg. We thank Professor Marcel Mayor for generous support of our research at the University of Basel, Switzerland, Professor Petr Klán from Masaryk University in Brno, Czech Republic for making available to us the infrastructure in his laboratory to perform the UV–Vis kinetic measurements, and Professor Josef Michl from University of Colorado Boulder, United States and Professor Bernd Engels from the University of Würzburg, Germany for useful discussions. Work at Georgetown was partially supported by an NSF grant (CHE-1006702).

REFERENCES

(1) (a) Woodward, R. B.; Hoffmann, R. *The Conservation of Orbital Symmetry*; Verlag Chemie: Weinheim, 1970. (b) Fleming, I. *Molecular Orbitals and Organic Chemical Reactions*; John Wiley and Sons: Chichester, 2010; pp. 253–368. (c) *Comprehensive Organic Synthesis*; Trost, B. M., Ed.; Pergamon Press: Oxford, 1991; Vol. 5. (d) Epiotis, N. D. *Angew. Chem. Int. Ed. Engl.* **1974**, *13*, 751–828. (e) Dewar, M. J. S. *Angew. Chem. Int. Ed. Engl.* **1971**, *10*, 761–870.

(2) (a) Seeman, J. I. *J. Org. Chem.* **2015**, *80*, 11632–11671. (b) Hoffmann, R. *Angew. Chem. Int. Ed.* **2004**, *43*, 6586–6590. (c) Woodward, R. B.; Hoffmann, R. *Angew. Chem. Int. Ed.* **1969**, *8*, 781–932. (d) Hoffmann, R.; Woodward, R. B. *Acc. Chem. Res.* **1968**, *1*, 17–22. (e) Longuet-Higgins, H. C.; Abrahamson, W. *J. Am. Chem. Soc.* **1965**, *87*, 2045–2026. (f) Woodward, R. B.; Hoffmann, R. *J. Am. Chem. Soc.* **1965**, *87*, 295–397. (g) Havinga, E.; Schlatmann, J. L. M. A. *Tetrahedron* **1961**, *16*, 146–152.

(3) (a) Hasegawa, M.; Murakami, M. *J. Org. Chem.* **2007**, *72*, 3764–3769. (b) Srinivasan, R. *J. Am. Chem. Soc.* **1969**, *91*, 7557–7561. (c) Winter, R. E. K. *Tetrahedron Lett.* **1965**, *6*, 1207–1212.

(4) (a) Chapter 4 in ref. 1a. (b) Chapter 6 in ref. 1c. (c) Criegee, R.; Noll, K. *Liebigs Ann. Chem.* **1959**, *627*, 1–14. (d) Vogel, E. *Liebigs Ann. Chem.* **1958**, *615*, 14–21.

(5) Hickenboth, C. R.; Moore, J. S.; White, S. R.; Sottos, N. R.; Baudry, B.; Wilson, S. R. *Nature* **2007**, *446*, 423–427.

(6) (a) Yamamoto, K.; Ueda, T.; Yumioka, H.; Okamoto, Y.; Yoshida, T. *Chem. Lett.* **1984**, *13*, 1977–1978. (b) Ben-Bassat, J. M.; Ginsburg, D. *Tetrahedron* **1974**, *30*, 483–491. (c) Schmidt, W. *Tetrahedron Lett.* **1972**, *13*, 581–584. (d) Schmidt, W. *Helv. Chim. Acta* **1971**, *54*, 862–868. (e) Blattmann, H.-R.; Schmidt, W. *Tetrahedron* **1970**, *26*, 5885–5899. (f) Blattmann, H.-R.; Meuche, D.; Heilbronner, E.; Molyneux, R. J.; Boekelheide, V. *J. Am. Chem. Soc.* **1965**, *87*, 130–131.

(7) (a) Muszkat, K. A.; Schmidt, W. *Helv. Chim. Acta* **1971**, *54*, 1195–1207. (b) Muszkat, K. A.; Gegiou, D.; Fischer, E. *Chem. Commun.* **1965**, 447–448.

(8) (a) Steiner, R. P.; Michl, J. *J. Am. Chem. Soc.* **1978**, *100*, 6413–6415. (b) Kolc, J.; Michl, J. *J. Am. Chem. Soc.* **1970**, *92*, 4147–4148.

(9) (a) Dolbier, Jr., W. R.; Matsui, K.; Dewey, H. J.; Horák, H. V.; Michl, J. *J. Am. Chem. Soc.* **1979**, *101*, 2136–2139. (b) Steiner, R. P.; Miller, R. D.; Dewey, H. J.; Michl, J. *J. Am. Chem. Soc.* **1979**, *101*, 1820–1826.

(10) (a) Uchida, K.; Ito, S.; Nakano, M.; Abe, M.; Kubo, T. *J. Am. Chem. Soc.* **2016**, *138*, 2399–2410. (b) Pogodin, S.; Agranat, I. *J. Am. Chem. Soc.* **2003**, *125*, 12829–12835.

(11) (a) Ravat, P.; Šolomek, T.; Ribar, P.; Juríček, M. *Synlett* **2016**, *27*, 1613–1617. (b) Ravat, P.; Šolomek, T.; Rickhaus, M.; Häussinger, D.; Neuburger, M.; Baumgarten, M.; Juríček, M. *Angew. Chem., Int. Ed.* **2016**, *55*, 1183–1186.

(12) (a) Li, Y.; Heng, W.-K.; Lee, B. S.; Aratani, N.; Zafra, J. L.; Bao, N.; Lee, R.; Sung, Y. M.; Sun, Z.; Huang, K.-W.; Webster, R. D.; Lopez Navarrete, J. T.; Kim, D.; Osuka, A.; Casado, J.; Ding, J.; Wu, J. *J. Am. Chem. Soc.* **2012**, *134*, 14913–14922. (b) Connelly, N. G.; Geiger, W. E. *Chem. Rev.* **1996**, *96*, 877–910. (c) Vazquez, C.; Calabrese, J. C.; Dixon, D. A.; Miller, J. S. *J. Org. Chem.* **1993**, *58*, 65–81. (d) Loufty, R. O.; Hsiao, C. K.; Ong, B. S.; Keoshkerian, B. *Can. J. Chem.* **1984**, *62*, 1877–1885.

(13) Nunes, C. M.; Reva, I.; Pinho e Melo, T. M. V. D.; Fausto, R.; Šolomek, T.; Bally, T. *J. Am. Chem. Soc.* **2011**, *133*, 18911–18923.

(14) Levy, B.; Berthier, G. *Quant. Chem.* **1968**, *2*, 307–319.

(15) The CAS(2,2)/6-31G(d) relaxed potential energy surface scans of the C–C bond formation coordinate starting from various geometries close to that of the S_1/S_0 conical intersection in **3a** (Figure 3a; $d_{(C–C)}$ = 2.164Å) always tended to converge to geometries that belong to C_2 symmetry.

(16) Frisch, M. J.; Trucks, G. W.; Schlegel, H. B.; Scuseria, G. E.; Robb, M. A.; Cheeseman, J. R.; Scalmani, G.; Barone, V.; Petersson, G. A.; Nakatsuji, H.; Li, X.; Caricato, M.; Marenich, A. V.; Bloino, J.; Janesko, B. G.; Gomperts, R.; Mennucci, B.; Hratchian, H. P.; Ortiz, J. V.; Izmaylov, A. F.; Sonnenberg, J. L.; Williams-Young, D.; Ding, F.; Lipparini, F.; Egidi, F.; Goings, J.; Peng, B.; Petrone, A.; Henderson, T.; Ranasinghe, D.; Zakrzewski, V. G.; Gao, J.; Rega, N.; Zheng, G.; Liang, W.; Hada, M.; Ehara, M.; Toyota, K.; Fukuda, R.; Hasegawa, J.; Ishida, M.; Nakajima, T.; Honda, Y.; Kitao, O.; Nakai, H.; Vreven, T.; Throssell, K.; Montgomery, J. A., Jr.; Peralta, J. E.; Ogliaro, F.; Bearpark, M. J.; Heyd, J. J.; Brothers, E. N.; Kudin, K. N.; Staroverov, V. N.; Keith, T. A.; Kobayashi, R.; Normand, J.; Raghavachari, K.; Rendell, A. P.; Burant, J. C.; Iyengar, S. S.; Tomasi, J.; Cossi, M.; Millam, J. M.; Klene, M.; Adamo, C.; Cammi, R.;

Ochterski, J. W.; Martin, R. L.; Morokuma, K.; Farkas, O.; Foresman, J. B.; Fox, D. J. Gaussian 09, Revision D.01, Gaussian, Inc., Wallingford CT, **2009**.

(17) Werner, H.-J.; Knowles, P. J.; Knizia, G.; Manby, F. R.; Schütz, M.; Celani, P.; Korona, T.; Lindh, R.; Mitrushenkov, A.; Rauhut, G.; Shamasundar, K. R.; Adler, T. B.; Amos, R. D.; Bernhardsson, A.; Berning, A.; Cooper, D. L.; Deegan, M. J. O.; Dobbyn, A. J.; Eckert, F.; Goll, E.; Hampel, C.; Hesselmann, A.; Hetzer, G.; Hrenar, T.; Jansen, G.; Köppl, C.; Liu, Y.; Lloyd, A. W.; Mata, R. A.; May, A. J.; McNicholas, S. J.; Meyer, W.; Mura, M. E.; Nicklass, A.; O'Neill, D. P.; Palmieri, P.; Pflüger, K.; Pitzer, R.; Reiher, M.; Shiozaki, T.; Stoll, H.; Stone, A. J.; Tarroni, R.; Thorsteinsson, T.; Wang, M.; Wolf, A. MOLPRO, Version 2010.1, a package of *ab initio* programs, see http://www.molpro.net.